Biomedical Signal Processing and Control 68 (2021) 102597

Contents lists available at ScienceDirect

Biomedical Signal Processing and Control

journal homepage: www.elsevier.com/locate/bspc

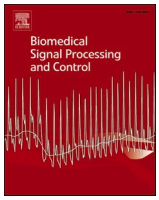

Identification of gait imagery based on fNIRS and class-dependent sparse representation

Hongquan Li [a], Anmin Gong [b], Lei Zhao [c], Fawang Wang [a], Qian Qian [a], Jianhua Zhou [a], Yunfa Fu [a,*]

[a] School of Automation and Information Engineering, Kunming University of Science and Technology, China
[b] Department of Information Engineering, Engineering University of Armed Police Force, China
[c] Faculty of Science, Kunming University of Science and Technology, China

ARTICLE INFO

Keywords:
Functional near infrared spectroscopy (fNIRS)
Class-dependent sparse representation classification (cdSRC)
Gait imagery
Abnormal gait after stroke
Combined features
Brain-computer interface (BCI)

ABSTRACT

The brain-computer interface (BCI) driven by gait imagery based on functional near-infrared spectroscopy (fNIRS) has potential applications in rehabilitation training for lower limb motor dysfunction, but its performance needs to be improved. The effectiveness of class-dependent sparse representation classification (cdSRC) for identifying gait imagery was explored in the study. First, fNIRS signals were collected from 15 subjects during gait imagery (normal gait imagery and abnormal gait imagery after stroke) and idle state. Mean value, peak value and root mean square of oxyhemoglobin (HbO) and their combinations were calculated as features for classification. Class-dependent *K*-nearest neighbor (cdKNN) and class-dependent orthogonal matching pursuit (cdOMP) were used to solve HbO features coded by sparse representation and classify them, and the classification results were compared with those obtained by support vector machine (SVM) and KNN. The experimental results showed that the average classification accuracy of three tasks by cdSRC using the combination features of mean value, peak value and root mean square was 87.39 ± 2.59%, which was significantly higher than those achieved by SVM and KNN (78.67 ± 3.96% and 79.78 ± 4.77%, respectively). We discovered that cdSRC combined with fNIRS could effectively identify gait imagery and also proved that the combined features of HbO had better separability than a single feature for gait imagery. Recognizing gait imagery based on fNIRS can be applied to BCI to provide new control commands. This type of BCI can provide active rehabilitation training methods for the disabled, such as providing control commands for mechanical prostheses so that the disabled can perform active rehabilitation training to restore some of their motor functions. In addition, to our knowledge, this study is the first to introduce cdSRC to identify gait imagery (three classes) based on fNIRS.

1. Introduction

Normal walking (normal gait) is completed by a series of activities of the pelvis, hips, knees, ankles and toes under the control of the central nervous system. It has certain stability, coordination, periodicity, and directionality. Normal gait can be obtained through learning, although it also has individual characteristics. Some diseases, such as a stroke, can significantly change the normal gait characteristics, causing the patient to have an abnormal gait.

After a stroke, the central nervous system of the patient suffers a certain amount of damage. The muscles relax at first, then the muscle tension gradually increases, and the movement of muscles and joints is limited to a certain extent. When walking, the upper limbs are often flexed and the lower limbs are straightened. Abnormal gait after stroke is often characterized by hip lifting, circle drawing and knee lifting, and the coordination and stability of the whole walking system is poor [1]. To overcome this abnormal gait, patients should not only develop good living habits in normal times but also perform long-term rehabilitation training for walking coordination dysfunction to improve gait. Among the rehabilitation training methods, active rehabilitation training based on brain-computer interface (BCI) has certain plasticity to the brain of stroke patients and is expected to improve the stability and coordination of their gait. Miao et al. used electroencephalograph (EEG) based on motor imagery to study the rehabilitation treatment of stroke patients. The results of the study showed that compared with traditional treatment methods, the more active rehabilitation treatment provided by the

* Corresponding author.
E-mail address: fyf@ynu.edu.cn (Y. Fu).

https://doi.org/10.1016/j.bspc.2021.102597
Received 2 August 2020; Received in revised form 23 March 2021; Accepted 26 March 2021
Available online 10 April 2021
1746-8094/

study can effectively restore the motor function of the upper extremities of stroke patients [2]. However, it is necessary to construct gait rehabilitation training methods based on BCI.

BCI is a revolutionary human-computer interaction. Among the many brain signals that drive BCI, EEG is the most widely used signal. Its temporal resolution is high, but its spatial resolution is low. It is also vulnerable to interference from artifacts such as electromagnetism, electrooculogram and motion induced electromyography. Compared with EEG, which measures the comprehensive discharge activity of neurons, functional near infrared spectroscopy (fNIRS) is a portable method for measuring cerebral blood oxygen metabolism. This method is not affected by electromagnetism or electrooculogram and can tolerate a certain degree of movement of the subject's head. It has a good ecological effect and is more suitable for dynamic monitoring of oxyhemoglobin (HbO) and deoxyhemoglobin (HbR) concentration changes in brain tissue during aerobic exercise and motor imagery [3]. Therefore, in this study, fNIRS is used to measure and identify the HbO and HbR concentrations during gait imagery (normal gait imagery and abnormal gait imagery after stroke) and idle state.

Currently, traditional machine learning and deep learning were often used to classify motor imagery based on fNIRS. Although traditional machine learning was simple, it was difficult to further improve the classification accuracy. Although deep learning had advantages in classification accuracy, with the deepening of the training network, the time required would also increase. Jin et al. extracted and combined the main feature channels during the tasks of the subjects' small-step with low-speed, small-step with mid-speed and mid-step with low-speed (ternary classification) and achieved an average classification accuracy of 78.79% using support vector machines (SVM) [4]. Therefore, this study introduced sparse representation classification (SRC) to decode gait imagery, which not only had higher classification accuracy but also required less time.

SRC has received widespread attention in the field of pattern recognition recently. In BCI based on EEG, SRC has been used for classification, and good results have been obtained. Himanshu et al. used weighted sparse representation classification (WSRC) to classify the data sets IVa and IIb of BCI Competition III and BCI Competition IV, with an average classification accuracy of 97.98% and 96% [5]. Huang et al. used an improved SRC to classify the above two competition data sets and further improved the classification accuracy to 98.82% [6]. However, the effectiveness of SRC in classifying fNIRS signals needs further verification.

This study is to further verify the effectiveness of SRC in classifying fNIRS signals on the basis of our previous study (binary classification) [7]. This study is the first time that SRC has been used to decode three classes of gait imagery, and it can be applied to BCI to provide new control commands. This type of BCI can bring good news to people with physical disabilities, such as providing control commands for artificial limbs so they can drink Coke.

2. Materials and methods

2.1. Subjects

A total of 17 healthy subjects (24 ± 5 years old) were recruited in the experiment. All of them had no history of mental, physical or psychological disorders. After explaining the experimental paradigm, verbal consents were obtained from all of the subjects. This experimental study was approved by the Academic Ethics Committee of Kunming University of Science and Technology and conducted in accordance with the latest Declaration of Helsinki.

2.2. Experimental paradigm and tasks

In the study, subjects performed three mental tasks: normal gait imagery, abnormal gait imagery after stroke and idle state. For normal gait imagery, subjects were required to imagine a normal gait from a first-person perspective, with a step length of 50–80 cm, a step width of 8 ± 3.5 cm and a step frequency of 95–125 steps / min. The lower limbs on both sides swung alternately, and the same process was repeated in the same periodicity or rhythmicity (the periodicity and rhythmicity of normal gait). All joints and muscles of the whole body participated in gait coordination. For abnormal gait imagery after stroke, the step length was less than 40 cm, and the step frequency was 32.1–85.3 steps / min. The time of double-leg support phase was longer than in normal gait, and the one-leg support phase of the healthy side was longer than that of the affected side and longer than in normal gait. Furthermore, the time of the swing phase of the affected side was longer than the time of the healthy side and longer than that of the normal gait. The specific performance was the joint movement of the flexor muscles (hip flexion and knee flexion) of the affected side at the beginning of the swing phase. The heel could not touch the ground at the end of the swing phase, the affected side could not bear weight when standing, the foot was turned inward and the walking was unstable. Normal gait imagery and abnormal gait imagery after stroke are shown in Fig. 1.

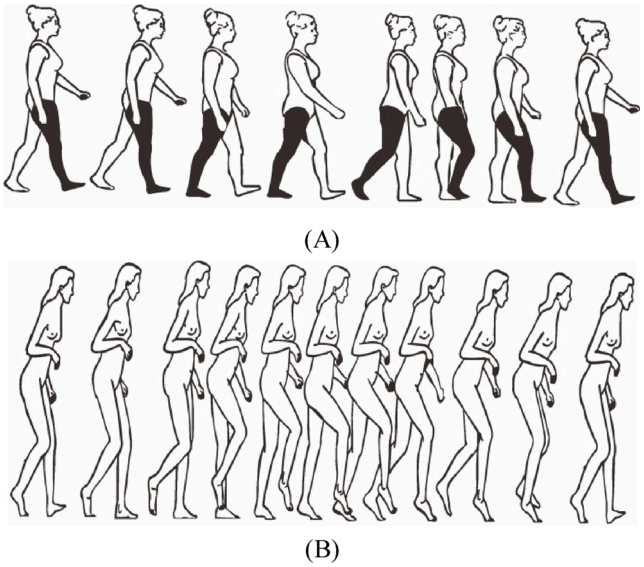

Fig. 1. Gait imagery, (A) normal gait imagery, (B) abnormal gait imagery after stroke.

At the beginning, the voice cues were: "baseline time, please stay awake and relaxed for 60 s." During this process, the subject was required not to perform specific mental tasks to keep the fNIRS signal at the baseline level. At the end of baseline time, the voice cue was "experimental task begins," followed by a randomly selected cue for one of the three tasks (normal gait imagery, abnormal gait imagery after stroke or idle state) in the form of voice; the whole cuing process lasted 2 s. After the task cue was over, the subject was asked to perform the cued task, and the whole task lasted for 10 s. At the end of the task, the voice cued "please take a rest", the resting time was 12 s. The above constituted one trial, and then the next trial would start. After the last trial, the voice cue was "resting state," requiring the subject to stay awake, close their eyes and relax for 180 s. The experimental paradigm was implemented by E-Prime (Psychology Software Tools, USA). There were 60 trials in each experiment and 20 trials in each task for about 30 min. Each subject conducted a total of 2 experiments with 40 trials for each task. The experimental paradigm of a single trial is shown in Fig. 2.

2.3. The subjects' gait imagery training

Effective gait imagery to produce the best results (measurement standard: vividness, clarity and controllability of kinesthetic imagery) is

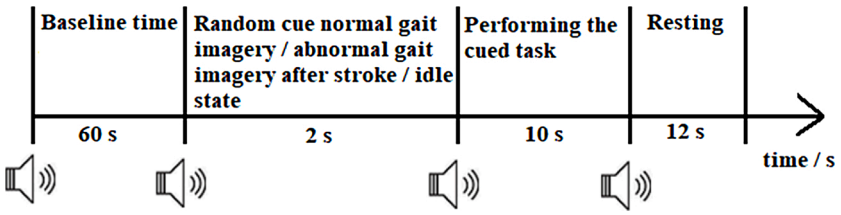

Fig. 2. The experimental paradigm of a single trial of gait imagery.

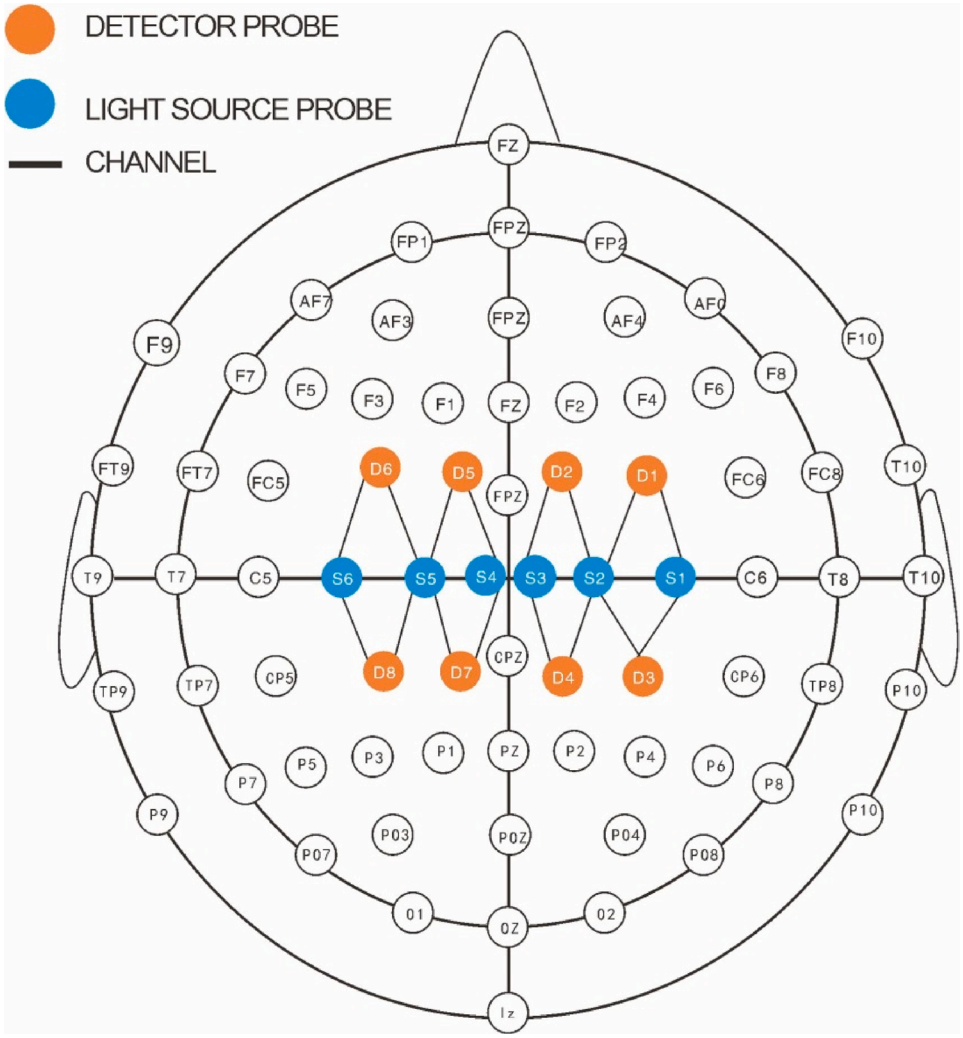

Fig. 3. The channel arrangement for data acquisition.

key to experimental research [8]. To this end, the subjects' gait imagery training was as follows:

2.3.1. Subjects' normal gait imagery training

First, the subjects were asked to walk in a normal gait to obtain the actual experience of the normal gait. Next, they performed kinesthetic imagery of the normal gait from the first-person perspective [8]. The subjects were instructed to focus on their own lower limbs instead of others' lower limbs, and to recall and feel their own walking process during motor imagery. They experienced a psychological rehearsal of walking without actual walking. Subjects may feel inhibited when they want to walk but are prevented from walking. They were asked to avoid performing visual gait imagery (i.e., seeing a walking movement picture in their brain). Each subject was trained until he or she reported that gait imagery was controllable and vivid.

2.3.2. Subjects' abnormal gait imagery training

First, let all subjects watch the action video of abnormal gait before the experiment; after watching the video, let the subject imitate the abnormal gait movement of the video; after training, two medical experts were invited to evaluate the abnormal gait movements of all subjects. Until both medical experts confirmed that the action was very close to an abnormal gait. Then, the subjects began to imagine abnormal gait based on the imitated movements. Until all the subjects reported that their abnormal gait imagery was almost the same as the video movements they watched. Finally, the experiment was officially launched after training and evaluation.

2.4. Equipment and data acquisition environment

The equipment used in this experiment is the fNIRS brain function

Fig. 4. The photo of the experimental paradigm of a subject's training for lower limb motor dysfunction.

imager Nirsmart (two wavelengths of 760 nm and 850 nm; 16 channels, China, Danyang Huichuang Medical Equipment Co., Ltd.). The channels were set according to the 10–20 international standard system [9]. The near-infrared probe covered the left and right motor areas of the brain, including eight channels in each of the left and right hemisphere of the brain, with the left and right regions arranged symmetrically. The sampling rate was 20 Hz, and the temporal resolution was 100 Hz. The channel arrangement for data acquisition is shown in Fig. 3.

The subjects were asked to perform the experiment in a quiet room with all lights turned off. The subjects sat on a chair about 1 m away from the computer screen and remained relaxed.

BCI measure brain activity, extract features from that activity, and convert those features into outputs that replace, restore, enhance, supplement, or improve human functions [10,11]. The fNIRS probes covering central motor areas in this study were placed according to the 10–20 international system. The distance between the light source probe and the detector probe of fNIRS was 3 cm. The layout of the light source probe and the detector probe is shown in Fig. 3. In the study, the original optical intensity data were converted into hemoglobin concentration data (HbO / HbR) by the modified Beer–Lambert law [12]. Fig. 4 is the experimental paradigm of the subject's training for lower limb motor dysfunction constructed for this study.

2.5. Data processing

2.5.1. fNIRS signal data preprocessing

The fNIRS signals included motion artifacts, physiological noises and baseline drift [13]. To improve the signal-to-noise ratio (SNR), the data needed to be preprocessed. First, the fNIRS signal was band-pass filtered with a frequency range of 0.02 Hz - 0.12 Hz to remove physiological noises. Then the Correlation-based signal improvement (CBSI) was used to remove motion artifacts caused by the subject's blinking and body shaking [14,15]. Finally, baseline drift correction was used to remove the baseline drift caused by the acquisition equipment and the subject's own state changes.

2.5.2. HbO signal feature extraction

After data preprocessing, the mean value, peak value and root mean square of HbO signals were extracted. They were considered as features alone and as combined features to identify gait imagery and idle state so as to find the features with the best classification effect.

The mean value represents the average HbO signal concentration of the subject during the task [16]. The expression for calculating the mean value is Eq. (1). Where N represents the total number of data samples, i_1 and i_2 represent the boundary of the data window during the task and i is the number of data samples during the task, HbO denotes HbO signals.

$$S_M = \frac{1}{N}\sum_{i=i_1}^{i_2} HbO(i) \tag{1}$$

The peak value represents the maximum HbO signal concentration of the subject during the task [17]. The peak value is the maximum value of the signal during the task, which depends on the boundaries i_1 and i_2 of the data window during the task.

The root mean square represents the effective HbO signal concentration of the subject during the task. The expression for calculating the root mean square is Eq. (2). Where N represents the total number of data samples, and i represents the i-th sampling point.

$$S_R = \sqrt{\frac{\sum_{i=1}^{N} HbO_i^2}{N}} \tag{2}$$

In this study, a total of 17 subjects participated in the experiment, and fNIRS data of 15 subjects (No. Sub1–Sub15) were analyzed. The data sets of the other two subjects were discarded due to personal reasons or equipment problems. The feature dimension of the data set during the task of each subject was 12000*16. In this experiment, the experimental data of each subject were randomly divided into a training set and a test set with the ratio of 8:2 and the range of all values were normalized to between -1 and 1.

2.6. Classification method

This study introduced class-dependent sparse representation classification (cdSRC) into fNIRS to identify gait imagery. Moreover, it was compared with the classification results of SVM and K-nearest neighbor (KNN) so as to verify the effectiveness of cdSRC in identifying gait imagery.

2.6.1. Class-dependent sparse representation classification (cdSRC)

In traditional sparse representation, test set samples can be linearly represented by a small number of training set samples of the same category. However, when sparsely representing the test set samples in a given dictionary, SRC will ignore the Euclidean distance relationship between samples [18].

To overcome the above shortcoming, cdSRC can be introduced. The cdSRC is mainly composed of the class-dependent orthogonal matching pursuit (cdOMP) algorithm and the class-dependent KNN (cdKNN) algorithm [19], which performs OMP and KNN in a class wise manner by incorporating the prior (class label) information. It effectively combines the ideas of SRC and KNN classifier in a class wise manner to exploit both correlation and Euclidean distance relationship between test and training samples. To achieve this goal, a unified class membership function is proposed, which uses both residual and Euclidean distance information. The class label of the test sample is not directly determined in cdOMP or cdKNN. Instead, a residual and a Euclidean distance between a test sample and the training samples in the dictionary are calculated via cdOMP and cdKNN, respectively [19]. The parameters of cdSRC are as follows: the sparsity level for cdSRC is 10, and the regularization parameter value of cdSRC is 0.05.

cdSRC algorithm:

Input:

Training data set $M = \{M_i\}_{i=1}^{c} \in \mathbb{R}^{d\times n}$, testing data set $y \in \mathbb{R}^{d}$, sparsity level is O, the number of nearest neighbors for KNN is K, the regularization parameter is λ.

(1) cdOMP. The cdOMP algorithm flow is as follows [20]:

Table 1
The average classification accuracy of cdSRC, SVM and KNN obtained under different features of HbO signal during normal gait imagery, abnormal gait imagery after stroke and idle state (three classes) of 15 subjects (%).

Classifier	Statistics type	Mean	Peak	RMS	M&P	M&R	P&R	M&P&R
cdSRC	Maximum accuracy	87.50	86.67	82.50	90.83	83.33	80.00	91.67
	Minimum accuracy	72.50	72.50	65.00	78.33	68.33	67.50	83.33
	Average accuracy	81.27	78.89	76.39	85.55	83.05	80.33	87.39
	±Std	±4.09	±4.02	±4.24	±3.04	±3.25	±3.93	±2.59
SVM	Maximum accuracy	79.17	75.83	76.67	81.67	76.67	75.00	86.67
	Minimum accuracy	53.33	50.00	49.17	67.50	60.00	65.00	72.5
	Average accuracy	67.02	64.94	58.50	74.56	72.22	68.12	78.67
	±Std	±7.86	±7.71	±8.70	±3.65	±4.74	±4.34	±3.96
KNN	Maximum accuracy	75.00	74.17	74.17	85.83	80.00	80.00	87.5
	Minimum accuracy	50.00	53.33	47.50	69.17	59.17	57.50	70.83
	Average accuracy	66.67	65.44	64.11	75.94	72.44	71.72	79.78
	±Std	±6.32	±5.50	±7.09	±4.34	±5.28	±5.51	±4.77

Std: Standard deviation.

(1) x represents the current signal and initializes the residual $e_0 = x$;
(2) Select the atom with the largest absolute value of the inner product with e_0, and express it as ϕ_1;
(3) Use the selected atoms as columns to form matrix Φ_t, and define the orthogonal projection operator of Φ_t column space

$$P = \Phi_t(\Phi_t^T\Phi_t)^{-1}\Phi_t^T \tag{3}$$

Obtain the residual e_1 by subtracting from e_0 its orthogonal projection onto the span of Φ_t:

$$e_1 = e_0 - Pe_0 = (I - P)e_0 \tag{4}$$

④ Iteratively execute Eqs. (3) and (4) on the residuals:

$$e_{m+1} = e_m - Pe_m = (I - P)e_m \tag{5}$$

Where I is the identity matrix.

The algorithm terminates when a specified stop rule is met.

(2) cdKNN. In cdKNN, the i th class distance is measured by the mean of Euclidean distances of the test sample and its K nearest neighbors. cdKNN is used to exploit the Euclidean distance information [19]. The algorithm flow of cdKNN is as follows:

For all $i \in 1,2,...,c$ do.

For all $j \in 1,2,...,n_i$ do.

Calculate the Euclidean distance D between y and x_{ij},

$$d_{ij} = D(y, x_{ij}). \tag{6}$$

End for

Calculate the mean of K minimum $\{d_{ij}\}_{j=1}^{n_i}$ as distance d_i of class i.

End for

Output:

Determine the class label l according to y:

$$l = \arg\min_{i=1,2,...,c}(y_i + \lambda d_i) \tag{7}$$

The class label of the training set M is l.

2.6.2. Support vector machine (SVM)

The basic idea of SVM is to maximize the distance (support vector) between the separation hyperplane and the nearest training sample, which shows good performance in both linear and nonlinear classification [21]. The basic type of SVM is:

$$\min_{\omega,b}\frac{1}{2}\left|\left|\omega\right|\right|^2 \quad s.t.\ \ vy_i(\omega^T x_i + b) \geq 1,\ \ i = 1,2,...,m. \tag{8}$$

Where $(x_i, y_i), i = 1, 2, ..., n$ are the training samples, ω is the normal vector, b is the displacement term.

In this study, SVM was used for the classification of gait imagery and compared with the classification results of cdSRC. The parameters of SVM were as follows: kernel function was RBF and gamma was 1; C was equal to 2; wi was equal to 1.05.

2.6.3. K-nearest neighbor (KNN)

The core idea of KNN is that if most of the K nearest samples of a sample in the feature space belongs to a certain category, it is determined that the sample also belongs to this category and has the characteristics of the sample in this category [22]. For an input training data set:

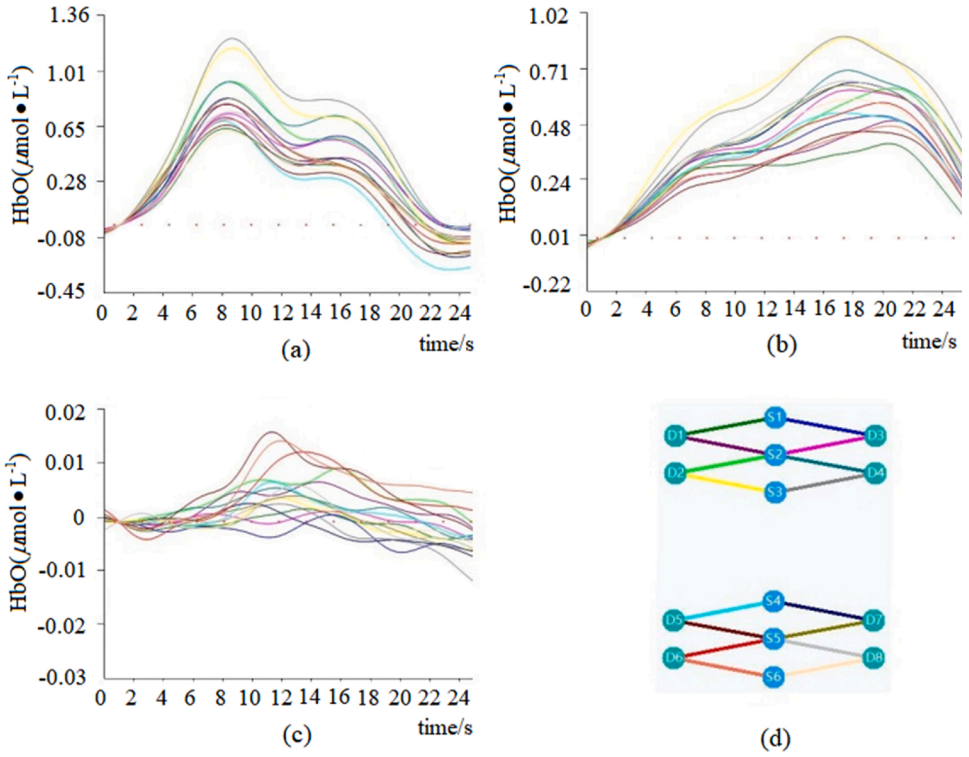

Fig. 5. The HbO signal concentration variation curve with time during the three tasks. (a) Normal gait imagery HbO signal concentration change curve. (b) Abnormal gait imagery after stroke HbO signal concentration change curve. (c) HbO signal concentration change curve in idle state. (d) Channels.

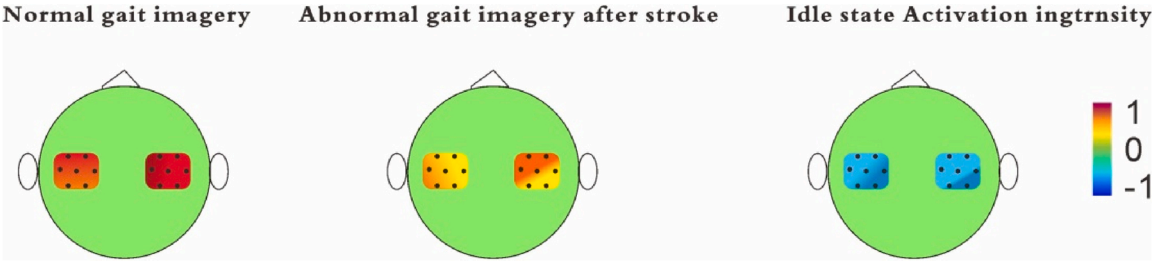

Fig. 6. Brain activation map of normal gait imagery, abnormal gait imagery after stroke and idle state.

$$M = \{(x_1, y_1), (x_2, y_2), ..., (x_N, y_N)\} \quad (9)$$

Where $x_i \in X \subseteq R^n$ is the instantiated feature vector, $y_i \in Y = \{c_1, c_2, ..., c_K\}$ is the instantiated category.

It can be seen from the above that the core idea of KNN is to find the K points closest to x in the input training set M.

In this study, KNN was used for the classification of gait imagery and compared with the classification results of cdSRC. The number of nearest neighbors for KNN was five.

3. Results

3.1. Classification results

Table 1 shows the average classification accuracy of 15 subjects when performing normal gait imagery, abnormal gait imagery after stroke and idle state using cdSRC, SVM and KNN to classify the different features of HbO signal. It can be seen from the table that for the three classifiers of cdSRC, SVM and KNN, the average classification accuracy obtained using the mean value (Mean, M) is higher than the peak value (Peak, P) and the root mean square (RMS, R). The average classification accuracies achieved by the three classifiers were 81.27 ± 4.08%, 67.02 ± 7.86% and 66.67 ± 6.32%, respectively. Among the combined features, the combination of mean value, peak value and root mean square achieved good classification accuracy in the three classifiers, that is, 87.39 ± 2.59%, 78.67 ± 3.96% and 79.78 ± 4.77%, respectively. It is particularly worth noting that cdSRC had higher average classification accuracy than SVM and KNN, regardless of single feature or combination of features.

3.2. HbO concentration response curves and brain activation map

Fig. 5 shows the HbO signal concentration variation curve with time during the three tasks, where the color of the curve corresponds to the channel. It can be seen from Fig. 5 that the time for the HbO concentration to reach the peak and the concentration value are different for different tasks. The time for the HbO signal concentration of normal gait imagery to reach the peak is about 7–9 s, and the average concentration value is about 0.80 μmol·L^{-1}. The time for the HbO signal concentration of abnormal gait imagery after stroke to reach the peak is about 13–15 s, and the average concentration value is about 0.55 μmol·L^{-1}. For the idle state, as the subjects remain awake and relaxed, the HbO signal concentration remains basically unchanged and the concentration value is around 0 μmol·L^{-1}. In addition, for both normal gait imagery and abnormal gait imagery after stroke, the HbO signal concentration begins

Table 2
Independent samples T test of normal gait imagery and abnormal gait imagery after stroke under different features.

Feature	Mean	Peak	RMS	M&P	M&R	P&R	M&P&R
Normal gait imagery mean value ±Std	0.412 ±0.09	0.701 ±0.13	0.723 ±0.11	0.697 ±0.07	0.686 ±0.09	0.479 ±0.10	0.872 ±0.14
Abnormal gait imagery mean value ±Std	0.256 ±0.11	0.448 ±0.15	0.544 ±0.13	0.375 ±0.10	0.457 ±0.12	0.358 ±0.14	0.401 ±0.16
t-value	0.982	0.735	0.814	2.264	1.458	1.212	2.651
p-value	0.016	0.035	0.021	0.0051	0.0082	0.013	0.002

Std: Standard deviation.

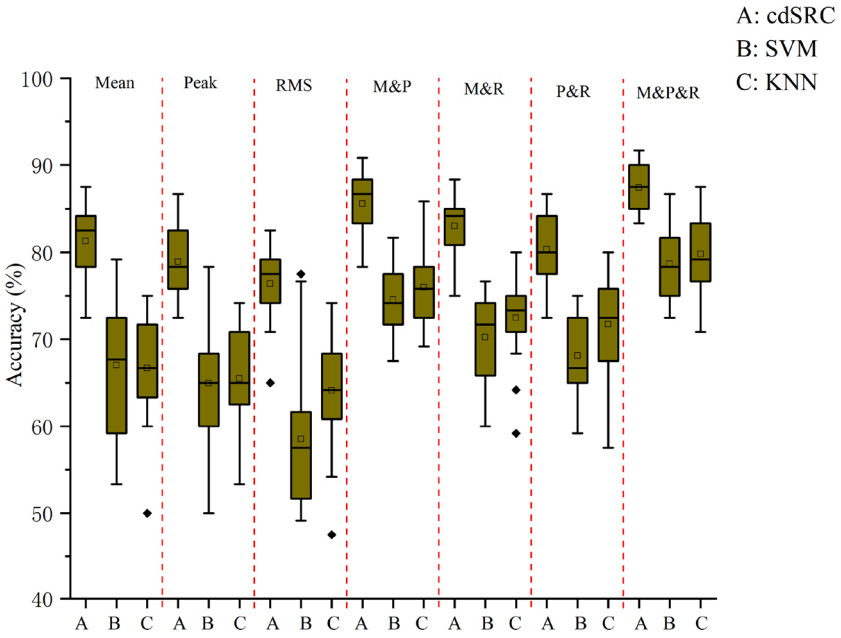

Fig. 7. Box plot comparison between cdSRC, SVM, and KNN classification accuracies.

to raise rapidly about 2 s after the start of the task. This is due to a time delay of about 2 s between the execution of mental activities and the HbO response [23]. The above analysis suggests that we can use the HbO signal change trend, peak value and time to peak value of different tasks as features to identify different tasks.

Fig. 6 shows the brain activation map of normal gait imagery, abnormal gait imagery after stroke and idle state. When performing normal gait imagery, the left and right brain activation intensity are roughly the same; when performing abnormal gait imagery after stroke, the right brain activation intensity is slightly higher than that of the left brain; in the idle state, because the subject does not perform any mental tasks, so the left and right brains are not activated. However, there are differences in the intensity and pattern of HbO signal concentration activation during the three tasks.

In addition, there is a physiological difference between normal gait imagery and abnormal gait imagery after stroke. For example, when the subject performs the normal gait imagery, the force on both legs is almost equal, and the activation degree of the left and right motor areas of the brain is roughly equal; when the subjects performs the abnormal gait imagery after a stroke, the force on both legs is uneven, and the activation degree of the left and right motor areas of the brain is also different. Therefore, when classifying this kind of motor imagery, it can be classified according to this physiological difference.

The key of this study is whether normal gait imagery and abnormal gait imagery after stroke are separable. Because the step length of normal gait imagery and abnormal gait imagery after stroke are different, we can use this to explore whether they are separable. However, more importantly, it can be judged from the extracted features whether the normal gait imagery and the abnormal gait imagery after stroke are separable. Therefore, the independent samples T test can be used to verify whether normal gait imagery and abnormal gait imagery after stroke are separable under each feature. The results of the independent samples T test are shown in Table 2. All p values of the independent samples T test results are less than 0.05. If a small probability event occurred, it is necessary to overturn the original hypothesis, that is, there is a very significant difference between the normal gait imagery and the abnormal gait imagery after stroke under the extracted features.

3.3. Statistical analysis

First, the Kolmogorov-Smirnov test (KS test) is used to verify whether the test results satisfy the standard normal distribution. The test result found that the normal distribution was not satisfied (KS test, $p > 0.05$). Since the one-way analysis of variance (ANOVA) must satisfy both normal distribution and equal variance. Therefore, we considered using the non-parametric Kruskal-Wallis test (KW test).

The p-value of the KW test results of the classification accuracy of the three classifiers was less than 0.05. Therefore, there were significant differences between at least two classifiers. In order to test whether there were significant differences between cdSRC and any two classifiers, we also needed to perform Wilcoxon signed rank test.

The value of $p_1 = 0.00065$ and $p_2 = 0.00098$ were the results of Wilcoxon signed rank test conducted on the classification accuracies of cdSRC compared with those of SVM and KNN, respectively. Since all p values were less than 0.05, the classification accuracy of cdSRC was significantly different compared with SVM and KNN. The comparative

Table 3
Comparison between this study and other related studies.

Author	Classification number	Classification features	Classifier	Accuracy
Christian [26]	3	HbO slope value	LDA	78%
Kim [27]	3	HbO mean value	LDA	75.6%
Amad [28]	3	HbO mean value	LDA	65.9%
Nauman [29]	3	HbO mean value	SVM	87.8%
This study	3	Mean, peak and root mean square combinations of HbO	cdSRC	87.39%

results between classification accuracies of cdSRC, SVM, and KNN were presented in box plots in Fig. 7.

4. Discussions

Compared with EEG, fNIRS has certain advantages. It is a relatively new brain function imaging method that can measure the blood oxygen metabolism activity of brain tissue in a portable way and indirectly estimate the activity of brain neurons. Therefore, fNIRS can be used as a method to measure brain activity of BCI. This study intends to establish recognition of gait imagery (three classes) based on fNIRS and apply it to the BCI system for rehabilitation training of lower limb motor dysfunction.

Varsehi et al. studied the channel selection method based on EEG-BCI, only 8 channels were selected when classifying motor imagery tasks, and the classification accuracy was 93.08% [24]. Zhang et al. used a deep convolutional neural network (CNN) to decode motor imagery, and the classification accuracy was 84.19%, which was an increase of 10% on the original basis [25]. Although EEG-based BCI has mostly achieved good classification results, fNIRS is a relatively new brain imaging technology, and its application field and classification accuracy also need to be further improved. Constructing an effective motor imagery decoding models from fNIRS signals is essential for many applications, especially in the BCI field that requires precise control of auxiliary equipment. For example, patients with lower limb disabilities can use fNIRS signals to control the movement of the wheelchair; amputees can use fNIRS signals to control the movement of the cursor on the screen.

This study is based on fNIRS decoding three classes of gait imagery (normal gait imagery, abnormal gait imagery after stroke and idle state). Because the experimental paradigm is relatively new, the previous research has no similar experimental paradigm, so it can only be compared with other related research. Table 3 shows the comparison between this study and other related studies. In these studies, LDA and SVM are mainly used as classifiers, and different classifiers will affect the classification accuracy to different degrees. Compared with these studies, the cdSRC was introduced into fNIRS for the first time. Under the designed experimental paradigm (normal gait imagery, abnormal gait imagery after stroke and idle state), the combined features of HbO mean value, peak value and root mean square achieved an average classification accuracy of 87.39%.

5. Conclusions

This study is the first attempt to apply cdSRC to fNIRS to identify three classes of tasks: normal gait imagery, abnormal gait imagery after stroke and idle state. The results show that for the method with the combined features of mean value, peak value and RMS, the average classification accuracy is 87.39 $\pm$ 2.59%, significantly higher than that of SVM or KNN (which are 78.67 $\pm$ 3.96% and 79.78 $\pm$ 4.77%, respectively). This proves that the cdSRC can effectively identify gait imagery and idle state, and it is expected to provide a new classification method for this kind of BCI.

Our future research will aim to construct an online fNIRS-BCI system driven by leg lift imagery, leg drop imagery and idle state for rehabilitation training of lower limb motor dysfunction.

CRediT authorship contribution statement

Hongquan Li: Conceptualization, Methodology, Software, Data curation, Writing - original draft, Validation, Writing - review & editing. **Anmin Gong:** Conceptualization, Formal analysis, Investigation, Methodology, Writing - review & editing. **Lei Zhao:** Software, Visualization, Data curation. **Fawang Wang:** Conceptualization, Supervision. **Qian Qian:** Software, Visualization. **Jianhua Zhou:** Validation, Investigation. **Yunfa Fu:** Conceptualization, Funding acquisition, Methodology, Project administration, Resources.

Acknowledgments

This work was supported by the National Natural Science Foundation (NNSF) of China under Grant Nos. 61763022, 81771926, 81470084, 61463024, 62006246. None of the authors have potential conflicts of interest to be disclosed.

Declaration of Competing Interest

The authors declare that they have no conflicts of interest.

References

[1] L. Gong, Y. Liu, L. Yi, et al., Abnormal gait patterns in autism Spectrum disorder and their correlations with social impairments, Autism Res. (2021).
[2] Y. Miao, S. Chen, X. Zhang, et al., BCI-based rehabilitation on the stroke in sequela stage, Neural Plast. 2020 (1) (2020) 1–10.
[3] H. Jeong, M. Song, S. Oh, et al., in: Toward Comparison of Cortical Activation with Different Motor Learning Methods Using Event-Related Design: EEG-fNIRS Study [C]//2019 41st Annual International Conference of the IEEE Engineering in Medicine and Biology Society (EMBC), IEEE, 2019, pp. 6339–6342.
[4] H. Jin, C. Li, J. Xu, Pilot study on gait classification using fNIRS signals, Comput. Intell. Neurosci. 2018 (2018) 1–9.
[5] S.R. Sreeja, D. Samanta, Distance-based weighted sparse representation to classify motor imagery EEG signals for BCI applications, Multimed. Tools Appl. (2020) 1–19.
[6] J.S. Huang, Y. Li, B.Q. Chen, et al., An intelligent EEG classification methodology based on sparse representation enhanced deep learning networks, Front. Neurosci. 14 (2020) 808.
[7] H. Li, A. Gong, L. Zhao, et al., Decoding of walking imagery and idle state using sparse representation based on fNIRS, Comput. Intell. Neurosci. 2021 (1) (2021) 1–10.
[8] R. Roberts, N. Callow, L. Hardy, et al., Movement imagery ability: development and assessment of a revised version of the vividness of movement imagery questionnaire, J. Sport Exerc. Psychol. 30 (2) (2008) 200–221.
[9] S.A. Balart-Sanchez, H. Velez-Perez, S. Rivera-Tello, et al., A step forward in the quest for a mobile EEG-designed epoch for psychophysiological studies, Biomedizinische Technik 64 (6) (2019) 655–667.
[10] U. Asgher, K. Khalil, M.J. Khan, et al., Enhanced accuracy for multiclass mental workload detection using long short-term memory for brain–computer interface, Front. Neursci. 14 (2020) 584.
[11] P.C. Petrantonakis, I. Kompatsiaris, Single-trial NIRS data classification for brain-computer interfaces using graph signal processing, IEEE Trans. Neural Syst. Rehabil. Eng. 26 (9) (2018) 1700–1709.
[12] R. Nishiyori, S. Bisconti, B. Ulrich, Motor cortex activity during functional motor skills: an fNIRS study, Brain Topogr. 29 (1) (2016) 42–55.
[13] E. Kirilina, A. Jelzow, A. Heine, et al., The physiological origin of task-evoked systemic artefacts in functional near infrared spectroscopy, Neuroimage 61 (1) (2012) 70–81.
[14] X. Cui, S. Bray, A.L. Reiss, Functional near infrared spectroscopy (NIRS) signal improvement based on negative correlation between oxygenated and deoxygenated hemoglobin dynamics, Neuroimage 49 (4) (2010) 3039–3046.
[15] A. Janani, M. Sasikala, Investigation of different approaches for noise reduction in functional near-infrared spectroscopy signals for brain–computer interface applications, Neural Comput. Appl. 28 (10) (2017) 2889–2903.
[16] Eda Akman Aydin, Subject-Specific feature selection for near infrared spectroscopy based brain-computer interfaces, Comput. Methods Prog. Biomed. 195 (2020), 105535.
[17] M.N.A. Khan, M.R. Bhutta, K.S. Hong, Task-specific stimulation duration for fNIRS brain-computer interface, IEEE Access 8 (2020) 89093–89105.

[18] J. Cao, K. Zhang, M. Luo, et al., Extreme learning machine and adaptive sparse representation for image classification, Neural Netw. 81 (2016) 91–102.
[19] M. Cui, S. Prasad, Class-dependent sparse representation classifier for robust hyperspectral image classification, Geosci. Remote Sens. IEEE Trans. 53 (5) (2015) 2683–2695.
[20] T.T. Cai, L. Wang, Orthogonal matching pursuit for sparse signal recovery with noise, IEEE Trans. Inf. Theory 57 (7) (2011) 4680–4688.
[21] K. Shankar, S.K. Lakshmanaprabu, D. Gupta, et al., Optimal feature-based multi-kernel SVM approach for thyroid disease classification, J. Supercomput. 76 (2) (2020) 1128–1143.
[22] X. Linquan, Z. Nan, X.U. Hao, et al., KNN nearest neighbor filling algorithm based on attribute correlation, J. Jiangxi Univ. Sci. Technol. 40 (01) (2019) 95–101.
[23] N. Naseer, K.S. Hong, Classification of functional near-infrared spectroscopy signals corresponding to the right- and left-wrist motor imagery for development of a brain-computer interface, Neurosci. Lett. 553 (2013) 84–89.
[24] H. Varsehi, S.M.P. Firoozabadi, An EEG channel selection metho for motor imagery based brain–computer interface and neurofeedback using Granger causality, Neural Netw. 133 (2021) 193–206.
[25] Kaishuo Zhang, et al., Adaptive transfer learning for EEG motor imagery classification with deep convolutional neural network, Neural Netw. 136 (2021) 1–10.
[26] H. Christian, H. Dominic, F. Ole, et al., Mental workload during n-back task—quantified in the prefrontal cortex using fNIRS, Front. Hum. Neurosci. 7 (2013) 935.
[27] K.S. Hong, N. Naseer, Y.H. Kim, Classification of prefrontal and motor cortex signals for three-class fNIRS-BCI, Neurosci. Lett. 587 (2015) 87–92.
[28] A. Zafar, K.S. Hong, Detection and classification of three-class initial dips from prefrontal cortex, Biomed. Opt. Express 8 (1) (2017) 367–383.
[29] N.K. Qureshi, N. Naseer, F.M. Noori, et al., Enhancing classification performance of functional near-infrared spectroscopy-brain–computer interface using adaptive estimation of general linear model coefficients, Front. Neurorobot. 11 (2017) 33.